The ER luminal C-terminus of AtSec62 is critical for male fertility and plant growth in *Arabidopsis thaliana*

Melanie Jasmine Mitterreiter, Franziska Annamaria Bosch, Thomas Brylok and Serena Schwenkert* (iD)

Department Biology I, Plant Sciences, Ludwig-Maximilians-Universität München, Großhaderner Straße 2-4, 82152 Planegg-Martinsried, Germany

*For correspondence (e-mail serena.schwenkert@lmu.de).

SUMMARY

Protein translocation into the endoplasmic reticulum (ER) occurs either co- or post-translationally through the Sec translocation system. The *Arabidopsis* Sec post-translocon is composed of the protein-conducting Sec61 complex, the chaperone-docking protein AtTPR7, the J-domain-containing proteins AtERdj2A/B and the yet uncharacterized AtSec62. Yeast Sec62p is suggested to mainly function in post-translational translocation, whereas mammalian Sec62 also interacts with ribosomes. In *Arabidopsis*, loss of AtSec62 leads to impaired growth and drastically reduced male fertility indicating the importance of AtSec62 in protein translocation and subsequent secretion in male gametophyte development. Moreover, AtSec62 seems to be divergent in function as compared with yeast Sec62p, since we were not able to complement the thermosensitive yeast mutant *sec62-ts*. Interestingly, AtSec62 has an additional third transmembrane domain in contrast to its yeast and mammalian counterparts resulting in an altered topology with the C-terminus facing the ER lumen instead of the cytosol. In addition, the AtSec62 C-terminus has proven to be indispensable for AtSec62 function, since a construct lacking the C-terminal region was not able to rescue the mutant phenotype in *Arabidopsis*. We thus propose that Sec62 acquired a unique topology and function in protein translocation into the ER in plants.

Keywords: AtSec62, Sec translocon, post-translational translocation, endoplasmic reticulum, male fertility, *Arabidopsis thaliana*.

INTRODUCTION

Membrane as well as secretory proteins are synthesized on cytosolic ribosomes and need to be transported across or into the endoplasmic reticulum (ER) membrane for processing and for further transport through the Golgi apparatus. Translocation of pre-proteins can occur either co-translationally or in a post-translational manner (reviewed by Rapoport, 2007; Cross *et al.*, 2009; Zimmermann *et al.*, 2011; Linxweiler *et al.*, 2017).

Co-translational protein transport into the ER involves the signal recognition particle (SRP) which is binding to the N-terminal signal sequence of the emerging polypeptide chain at the ribosomes thereby arresting elongation (Saraogi and Shan, 2011). Subsequently, the SRP binds the SRP receptor which is localized to the ER membrane and is composed of the soluble subunit SRα and the membrane anchoring SRβ (Tajima *et al.*, 1986; Schwartz and Blobel, 2003). Binding of the SRP to its receptor enables an interaction of the ribosome, still harbouring the nascent

polypeptide chain, and the Sec translocation complex (Saraogi and Shan, 2011). Translation continues after dissociation of the SRP, while the emerging polypeptide is simultaneously translocated through the Sec61 channel (Saraogi and Shan, 2011).

However, most small pre-secretory proteins in yeast and mammals are imported post-translationally due to their signal sequence being transcribed only shortly before protein translation is entirely completed (Lakkaraju *et al.*, 2012; Ast and Schuldiner, 2013). Fully translated pre-proteins are bound by cytosolic chaperones including heat shock proteins (HSPs) like HSP70, which prevent molecular crowding as well as premature folding of the polypeptide and facilitate guidance of the pre-protein to the Sec translocation complex (Zimmermann *et al.*, 1988; Ng *et al.*, 1996; Ngosuwan *et al.*, 2003). In yeast, the Sec translocon is composed of the heterotrimeric complex Sec61 (composed of Sec61p, Sbh1p and Sss1p) forming the translocation channel and a tetrameric complex of Sec62p, Sec63p,

Sec71p and Sec72p (Deshaies *et al.*, 1991; Panzner *et al.*, 1995; Harada *et al.*, 2011). The Sec61 complex and Sec63p are involved in co-and post-translational protein translocation, whereas Sec62p, Sec71p and Sec72p are associated with post-translational translocation only (Deshaies *et al.*, 1991; Brodsky and Schekman, 1993; Panzner *et al.*, 1995). Together, Sec62p, Sec71p and Sec72p, probably act as a signal peptide receptor with Sec72p enabling interaction through its tetratricopeptide repeat (TPR) domain (Fang and Green, 1994; Feldheim and Schekman, 1994; Lyman and Schekman, 1997; Plath *et al.*, 1998; Schlegel *et al.*, 2007). Moreover, Yim *et al.* (2018) proposed that Sec62p, Sec63p, Sec71p and Sec72p associate in different combinations depending on the signal sequence characteristics of the translocation substrate. The positively charged Sec62p N-terminus is important for its interaction with Sec63p (Wittke *et al.*, 2000; Willer *et al.*, 2003; Müller *et al.*, 2010; Jung *et al.*, 2014) and recent studies even suggested a role for the Sec62p–Sec63p complex in membrane protein insertion and topogenesis of signal anchor proteins (Reithinger *et al.*, 2013; Jung *et al.*, 2014, 2019). Moreover, the Sec62p–Sec63p complex has been shown to interact with Sec61 through Sec63p thereby causing lateral channel opening and activating Sec61 for post-translational protein translocation (Harada *et al.*, 2011; Itskanov and Park, 2019; Wu *et al.*, 2019). For successful import into the ER the luminal HSP70-like chaperone Kar2p/BiP binds to the polypeptide chain, while it is still translocated by Sec61 to prevent it from sliding back into the cytosol (Brodsky and Schekman, 1993; Brodsky *et al.*, 1995; Panzner *et al.*, 1995; Osborne *et al.*, 2005; Rapoport, 2007). For this purpose, Kar2p/BiP interacts with the J-domain of Sec63p activating its ATPase domain and thereby closing its peptide binding pocket (Brodsky and Schekman, 1993; Brodsky *et al.*, 1995; Osborne *et al.*, 2005; Rapoport, 2007). After complete translocation, peptide-bound Kar2p/BiP is released by ADP-ATP exchange (Osborne *et al.*, 2005; Rapoport, 2007).

For mammalian cells, favouring co-translational protein import, the homologous Sec62 has been shown to be interacting with the ribosomal exit tunnel, suggesting a role of Sec62 in co-translational protein transport as well and therefore a gain of function in comparison with its yeast homologue (Müller *et al.*, 2010). This interaction is enabled by two oligopeptide motifs that are exclusively found in mammalian Sec62 but not in its yeast or plant homologues (Müller *et al.*, 2010). Nevertheless, Lang *et al.* (2012) demonstrated that silencing of *SEC62* impairs the post-translational import of a small, pre-secretory protein into the human ER, while co-translational translocation as well as post-translational insertion of tail-anchored proteins remained unaffected indicating that ribosome binding of Sec62 might only be relevant in coordinating protein translocation across the ER membrane. Furthermore, Lakkaraju *et al.* (2012) found that mammalian Sec62

ensures efficient post-translational translocation of proteins shorter than around 160 amino acids and is crucial for proteins up to a length of 100 amino acids. Mammalian Sec62 and Sec63 are associated with the Sec61 channel (Meyer *et al.*, 2000; Tyedmers *et al.*, 2000) (composed of Sec61α, Sec61β and Sec61γ being the mammalian homologues of Sec61p, Sbh1p and Sss1p, compare with Martínez-Gil *et al.*, 2011) and might also be involved in recruiting BiP as well as translocation substrates to the translocon (Müller *et al.*, 2010; Lakkaraju *et al.*, 2012). The interaction between Sec62 and Sec61 is Ca^{2+}-sensitive and mammalian Sec62, possessing a potential C-terminal EF hand motif, is important for Ca^{2+} homeostasis (Linxweiler *et al.*, 2013). An additional role of Sec62 in stress recovery has recently been shown by demonstrating that a C-terminal region of human Sec62 is required for delivering ER proteins to the autolysosomal system (Fumagalli *et al.*, 2016).

However, there is only scarce knowledge concerning the ER protein translocation in plants. The *Arabidopsis thaliana* genome encodes three isoforms of the channel-forming Sec61α homologue, two isoforms of the Sec63 homologue, named AtERdj2A and AtERdj2B (Yamamoto *et al.*, 2008), but only one Sec62 homologue (Schweiger and Schwenkert, 2013). Yamamoto *et al.* (2008) demonstrated the importance of AtERdj2A in protein translocation reflected by drastic pollen germination defects in the respective T-DNA insertion line probably due to defective protein secretion, whereas AtERdj2B was proposed to have an auxiliary role only. Interestingly, neither AtERdj2A nor AtERdj2B was able to rescue the thermosensitive growth phenotype of the respective yeast mutant (Yamamoto *et al.*, 2008). The ER localized TPR protein AtTPR7 has recently been described and its interaction with the cytosolic chaperones HSP70 and HSP90 was demonstrated, implying a role in guiding pre-proteins to the Sec post-translocon (Schweiger *et al.*, 2012, 2013; Schweiger and Schwenkert, 2013). Strikingly, AtTPR7 was able to restore post-translational protein import in a *Δsec71* yeast knockout mutant and was proposed to functionally replace Sec71p and the TPR protein Sec72p (Schweiger *et al.*, 2012). An interaction between AtTPR7 and AtERdj2A/B as well as AtSec62 has additionally been shown providing further information regarding the composition of the *Arabidopsis* Sec post-translocon (Schweiger *et al.*, 2012; Schweiger and Schwenkert, 2013).

In this study, we characterize the ER membrane localized protein AtSec62 (At3g20920), which shares only 12% sequence identity with yeast Sec62p and 15% with its mammalian counterpart (Schweiger and Schwenkert, 2013). We demonstrate that AtSec62 interestingly has a third transmembrane domain in contrast with its yeast and mammalian homologues (Deshaies and Schekman, 1989, 1990; Müller *et al.*, 2010) resulting in its C-terminus being

exposed to the ER lumen. The *atsec62* T-DNA insertion line displays defects in pollen development and pollen tube germination implying an important role of AtSec62 for male fertility probably due to influencing protein secretion similar to AtERdj2A (Yamamoto *et al.*, 2008). Furthermore, we show that AtSec62 is not able to rescue the thermosensitive growth phenotype of the respective *sec62-ts* yeast mutant and that its C-terminus is essential for AtSec62 function. We therefore propose that the AtSec62 C-terminus acquired a unique function in plants and that AtSec62, as part of the Sec post-translocon in *Arabidopsis*, is critical for plant growth and male fertility.

RESULTS

atsec62 displays vegetative and generative growth defects

We identified an *atsec62* T-DNA insertion line with an insertion in exon 1 of *AtSEC62* and homozygous mutant plants were selected by PCR using the oligonucleotides *AtSEC62*-5′UTR-f, *AtSEC62*-Exon2-r and Gabi-LB8409 (Figure 1a,b). Even though no obvious aerial phenotype was observable during initial growth, *atsec62* plants clearly displayed an impaired growth in comparison with wild-type plants after 4 weeks (Figure 1c). However, 2-week-old *atsec62* seedlings already showed an altered root morphology in contrast with Col-0 with their primary root length being reduced by 31% but a nearly 50% increase regarding the number of lateral roots (Figure S1). RNA was extracted

from leaves of 4-week-old plants and the absence of *AtSEC62* transcript in *atsec62* was confirmed by RT-PCR (Figure 1d). Immunodetection using an AtSec62 specific antibody also revealed the absence of AtSec62 protein in microsomal membranes isolated from *atsec62* leaves (Figure 1e). For complementation analysis, we generated a construct coding for the full-length *AtSEC62* under the control of the endogenous promoter. Following stable transformation and selection of plants, we isolated two lines of homozygous *atsec62* plants carrying the construct coding for endogenous *AtSEC62*, *pAtSEC62::AtSEC62 #14-6* and *pAtSEC62::AtSEC62 #27-2* (Figure 1b,d). In both lines, the *atsec62* growth phenotype was completely rescued by expression of endogenous AtSec62 (Figure 1c).

During initial screening for *atsec62* plants, we observed a very low number of homozygous mutant plants and consequently examined the segregation pattern of progeny plants derived from heterozygous *atsec62* plants (+/−). Normal Mendelian segregation would imply 50% heterozygous progeny, 25% wild-type and 25% homozygous progeny. Interestingly, plants displayed only 8.83% homozygous progeny, but 40.38% wild-type and 50.79% heterozygous progeny (*n* = 317), significantly differing from the expected ratio (Table 1a). When grown on half-strength Murashige and Skoog (½MS) medium containing 10 μg ml^{-1} sulfadiazine, only plants carrying the T-DNA insertion should be resistant, resulting in 75% of resistant progeny plants derived from *atsec62* (+/−). However, we observed only
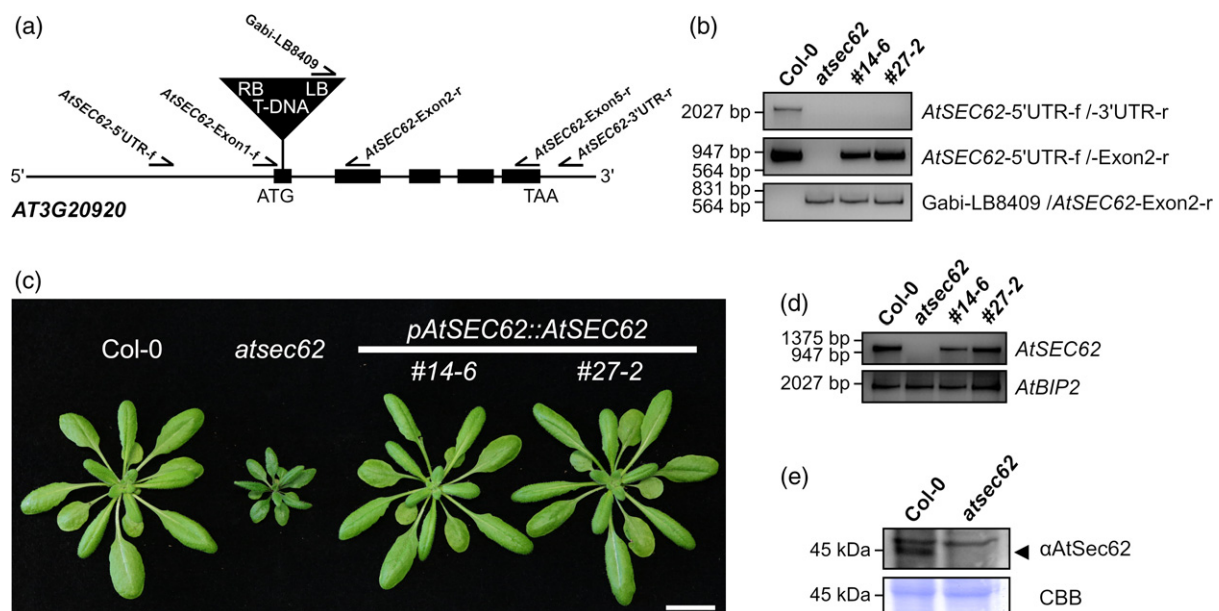
Figure 1. *atsec62* T-DNA insertion line and complementation. (a) *AT3G20920* (*AtSEC62*) gene structure and location of the T-DNA insertion in exon 1, also indicating the T-DNA left (LB) and right border (RB). (b) Genotyping PCR using the oligonucleotides *AtSEC62*-5′UTR-f, *AtSEC62*-Exon2-r and Gabi-LB8409. Oligonucleotide binding sites in *AtSEC62* are indicated in (a). (c) Phenotyping of 4-week-old plants of the *atsec62* T-DNA insertion line and the complemented lines *pAtSEC62::AtSEC62 #14-6* (*#14-6*) as well as *pAtSEC62::AtSEC62 #27-2* (*#27-2*) in comparison with Col-0. Scale bar represents 2 cm. (d) RT-PCR for *AtSEC62* and the control *AtBIP2*. Oligonucleotide binding sites for *AtSEC62*-Exon1-f and *AtSEC62*-Exon5-r in *AtSEC62* are indicated in (a). (e) Immunodetection of Col-0 and *atsec62* microsomal membranes using an AtSec62 antibody (upper panel) and Coomassie stain (lower panel).

Table 1 Segregation analysis for heterozygous *atsec62* (+/−) plants. (a) Segregation of *atsec62* (+/−) in comparison with Col-0 and *pAtSEC62::AtSEC62 #14-6* (*#14-6*) as well as *pAtSEC62:: AtSEC62 #27-2* (*#27-2*). Progeny genotype was determined by PCR using *AtSEC62* and T-DNA specific oligonucleotides. (b) Segregation on sulfadiazine (10 μg ml^{-1}) was examined by investigating the number of resistant (Sulfa^R) and sensitive (Sulfa^S) plants. *P*-value for expected segregation, validation by chi-squared analysis

(a) Segregation

Genotype	Wild-type progeny	Heterozygous progeny	Homozygous progeny	$p_{1:2:1}$
atsec62 (+/-)	128	161	28	1.92×10^{-4}

(b) Segregation on sulfadiazine

Genotype	Sulfa^R	Sulfa^S	Sulfa^R [%]	$p_{3:1}$	$p_{1:1}$	$p_{3:2}$
Col-0	0	100	0	–	–	–
atsec62 (+/-)	163	115	58.63	2.94×10^{-10}	0.0040	0.6418
#14-6	98	0	100	–	–	–
#27-2	103	0	100	–	–	–

58.63% and therefore assumed that the transmission of the *AtSEC62* mutation was affected (Table 1b). Male or female gametophyte mutants typically display a segregation ratio of 1:1 (Liu and Qu, 2008; Drews and Koltunow, 2011), but progeny plants derived from *atsec62* (+/−) rather segregated in a 3:2 ratio (Table 1b).

Defects in pollen development and tube germination lead to decreased male fertility in *atsec62*

Besides the distorted segregation ratio, we observed aborted and mostly empty siliques for *atsec62* providing further evidence for a gametophytic defect in the mutant (Figure 2a). For further analysis of potential gametophytic defects, we examined the siliques of *atsec62* (+/−), which should display a reduced seed set or defective seeds if the female gametophyte was non-functional (Liu and Qu, 2008; Drews and Koltunow, 2011). As we observed no difference between wild-type siliques and those of heterozygous mutant plants, we conclude that female gametophytes in *atsec62* are still functional.

We then tested pollen viability by Alexander staining which allows discriminating between viable (violet staining) and non-functional, greenish pollen grains (Alexander, 1969). When staining anthers of opening buds, the majority of *atsec62* anthers appeared rather greenish with only occasionally faint violet staining and no pollen-like structures visible, whereas viable pollen grains were present in Col-0 and the complemented lines (Figure 2b). Strikingly, when staining anthers of already open flowers, corresponding to dehiscent wild-type anthers, we observed some pollen-like structures clustered together in *atsec62* anthers (Figure 2b). Besides general defects in pollen development probably resulting in coherent pollen-like structures, we therefore propose that in *atsec62* anther

and pollen development are severely delayed in comparison with the female gametophyte and therefore proper pollination does not occur. *In vitro* pollen germination was subsequently examined by incubating pollen grains on solid medium for 22 h at either 25°C or 37°C. Interestingly, less pollen were released from *atsec62* than from Col-0 anthers and the germination rate of *atsec62* pollen at 25°C was reduced by 57% in comparison to wild-type pollen, while mutant pollen were hardly germinating at 37°C (Table 2). We therefore assume that the absence of AtSec62 also has a great impact on pollen tube germination, which is likewise reflected in the expression pattern of *AtSEC62* with the highest expression being observed in the mature pollen (*Arabidopsis* eFP browser, http://bar.utoronto.ca/, Winter *et al.*, 2007). Due to defective pollen development and pollen tube germination, *atsec62* displays a drastically reduced male fertility resulting in only 3.79 ± 2.42 mg seeds/plant ($n = 28$) in comparison with Col-0 plants yielding 440.50 ± 26.33 mg seeds/plant ($n = 7$) (shown as mean ± SD, $P = 4.86 \times 10^{-40}$, compare with Figure 2c).

atsec62 is sensitive towards high-temperature and ER stress

For further investigation of heat sensitivity of *atsec62*, we conducted a high-temperature stress treatment according to Yang *et al.* (2009). Seeds on ½MS medium were stratified for 3 days at 4°C, germinated at 37°C for 48 h and then transferred to 22°C. Germination was monitored 5 days after stress treatment, while survival rate was determined after 12 days growth at 22°C. Without heat treatment, the germination rate of *atsec62* seeds is already reduced by 15% in comparison with Col-0 seeds, while there is no further effect on the germination rate upon high-temperature stress (Table 2). Whereas 25.96% of germinated *atsec62* plants suffered and died from the previous treatment, wild-type plants survived (Table 2). In addition to the reduced tolerance of *atsec62* against heat, we observed an increased susceptibility towards ER stress, when growing plants on ½MS medium containing dithiothreitol (DTT) (Figure S2).

AtSec62 localizes to the ER membrane and has three transmembrane domains

Besides its role during plant growth and development, we were interested in the orientation of AtSec62 within the ER membrane. It has recently been suggested that AtSec62 has a third predicted transmembrane domain (Schweiger and Schwenkert, 2013), which would alter its topology in comparison with its yeast and mammalian counterparts (Deshaies and Schekman, 1989, 1990; Müller *et al.*, 2010). For further investigation, we compared the amino acid sequences of different Sec62 homologues including higher plants (*A. thaliana*, *Oryza sativa* and *Zea mays*), the moss

Figure 2. Reduced male fertility in *atsec62*. (a) Siliques of *atsec62* in comparison with Col-0 and complemented lines *pAtSEC62::AtSEC62 #14-6* (*#14-6*) as well as *pAtSEC62::AtSEC62 #27-2* (*#27-2*). Scale bars represent 5 mm. (b) Alexander staining of anthers from opening buds or open flowers of Col-0, *atsec62* and the complemented lines *#14-6* and *#27-2*. Scale bars represent 100 μm. (c) Amount of Col-0 and *atsec62* seeds obtained from one plant. Scale bar represents 5 mm.
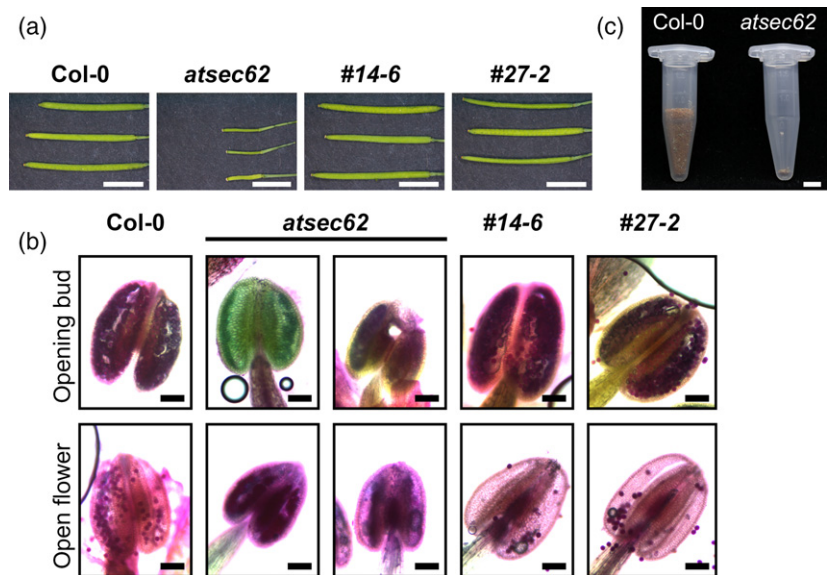
Table 2 Comparison of Col-0 and *atsec62* pollen tube germination, seed germination and survival upon high-temperature stress. Numbers indicate percentage of germinated pollen and seeds or percentage of germinated plants that survived high-temperature stress

Line	Pollen tube germination [%][a]		Seed germination [%][b]		Survival [%][c]	
	25°C	37°C	22°C	37°C	22°C	37°C
Col-0	24.56	15.78	97.80	96.12	100.00	99.24
atsec62	10.50	0.82	83.46	81.40	96.43	74.04

[a]Col-0 at 25°C ($n = 950$), Col-0 at 37°C ($n = 928$), *atsec62* at 25°C ($n = 203$), *atsec62* at 37°C ($n = 164$).
[b]Col-0 at 22°C ($n = 139$), Col-0 at 37°C ($n = 129$), *atsec62* at 22°C ($n = 133$), *atsec62* at 37°C ($n = 129$).
[c]Col-0 at 22°C ($n = 133$), Col-0 at 37°C ($n = 131$), *atsec62* at 22°C ($n = 112$), *atsec62* at 37°C ($n = 104$).

Physcomitrella patens, the unicellular green algae *Chlamydomonas reinhardtii* as well as mammals (*Homo sapiens* and *Mus musculus*), *Drosophila eugracilis* and yeast (*Saccharomyces cerevisiae*). Interestingly, AtSec62 shares only 12% and 15% sequence identity with its yeast and mammalian counterparts (Schweiger and Schwenkert, 2013). Two transmembrane domains were predicted for all analyzed Sec62 homologues, whereas a third transmembrane domain was only predicted for plant Sec62 containing many hydrophobic amino acids (Figure 3a, for complete sequence alignment see Figure S3). Furthermore, the C-terminal region of AtSec62 harbours predicted N-glycosylation sites with the consensus motif N-X-S/T (with X being any amino acid except proline) (compare with Marshall, 1972), which are absent in yeast and mammals (compare with Figure S3). We investigated AtSec62 topology by using the full-length AtSec62 as well as a truncated AtSec62 lacking the C-terminal region and the third transmembrane domain (Δ248−365), named AtSec62−ΔTMD3/C (Figure 3b).

We initially expressed N- and C-terminal GFP-fusion constructs in tobacco, named GFP−*AtSEC62* and *AtSEC62*−GFP, to test whether GFP-fusion would affect AtSec62 targeting and to confirm its ER localization. Both constructs and a construct coding for an ER marker protein fused to mCherry (compare with Nelson *et al.*, 2007) were transformed into *Agrobacterium* and bacterial cells carrying the respective constructs were co-infiltrated into tobacco leaves. Fluorescence was monitored in intact leaves or isolated protoplasts. Both GFP-fusion proteins were localized to the ER, indicating that fusion of a GFP-tag would not affect AtSec62 targeting (Figures 4a–c and S4).

To confirm the altered topology of AtSec62, we made use of a Split-GFP Gateway system including plasmids coding for cytosolic or ER luminal GFP1–10 (Xie *et al.*, 2017). In addition, we generated constructs with an N- or C-terminal fusion of the eleventh GFP β-sheet to AtSec62, named GFP11–AtSec62 and AtSec62–GFP11, or to AtSec62−ΔTMD3/C, named GFP11–AtSec62-ΔTMD3/C and AtSec62−ΔTMD3/C−GFP11. After co-infiltration into tobacco leaves, we detected fluorescent signals in intact leaves as well as in isolated protoplasts (Figures 4d and S5). Only upon co-expression with the cytosolic GFP1–10, there was an ER localized fluorescent signal detectable for GFP11−AtSec62, whereas fluorescence for AtSec62−GFP11 was only observable when co-expressed with the ER luminal GFP1–10−HDEL. In contrast, GFP11−AtSec62−ΔTMD3/C and AtSec62−ΔTMD3/C−GFP11 produced a detectable signal only with cytosolic GFP1–10. We therefore demonstrated that AtSec62 has three transmembrane domains
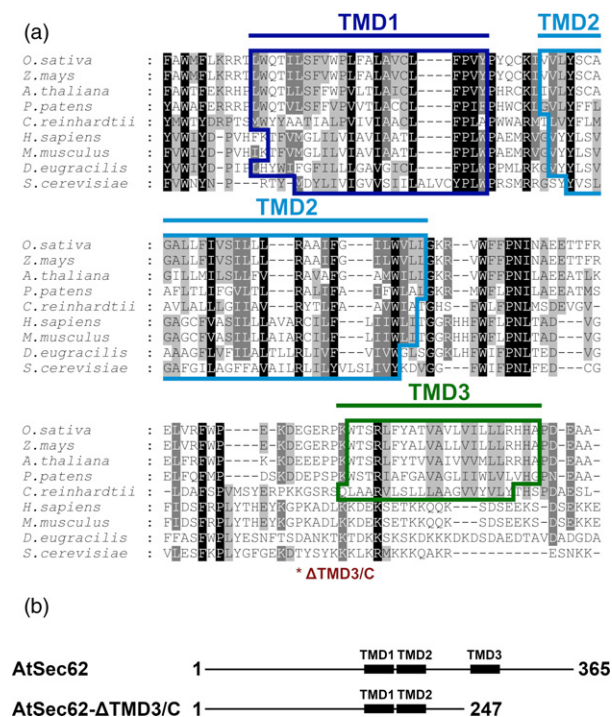
Figure 3. Predicted transmembrane domains for Sec62 homologues and AtSec62 constructs. (a) Alignment of AtSec62 with homologues of *O. sativa*, *Z. mays*, *P. patens*, *C. reinhardtii*, *H. sapiens*, *M. musculus*, *D. eugracilis* and *S. cerevisiae*. Conserved amino acids are shaded in black/grey. Predicted transmembrane domains (TMD) are indicated in dark blue (TMD1), light blue (TMD2) and green (TMD3). (b) Scheme of AtSec62 (amino acids 1–365) and AtSec62-ΔTMD3/C (amino acids 1–247) TMD organization. The inserted stop codon in AtSec62-ΔTMD3/C is indicated in red in (a).

resulting in its N-terminus facing the cytosol, while its C-terminus is located in the ER lumen (Figure 4e).

AtSec62 cannot rescue the growth phenotype of the yeast mutant *sec62-ts*

As we have shown that AtSec62 has an altered topology compared to its yeast homologue, we further tested whether AtSec62 and Sec62p are conserved on a functional level. For this purpose, we conducted complementation analysis using the thermosensitive yeast mutant *sec62-ts* and the wild-type strain W303. Due to a thermosensitive Sec62p version, normal growth of *sec62-ts* is only enabled at permissive temperature (28°C) but not at restrictive temperature (37°C). We tried to complement this mutant with full-length *AtSEC62*, *AtSEC62–ΔTMD3/C* as well as with endogenous Sec62p as positive control. Strikingly, growth of *sec62-ts* at 37°C was still inhibited for mutants carrying the construct coding for AtSec62 and AtSec62–ΔTMD3/C or the empty vector control, whereas growth was fully restored upon expression of the endogenous Sec62p (Figure 5a). The presence of *AtSEC62* and *AtSEC62–ΔTMD3/C* transcript was confirmed by RT-PCR (Figure 5b).

AtSec62 C-terminus is required for its function in plants

As the AtSec62 C-terminus is facing the ER lumen in contrast to yeast and mammalian Sec62 homologues, we were interested in whether the C-terminus has an essential function in protein translocation across the ER membrane in *Arabidopsis*. To investigate the role of the AtSec62 C-terminus, we performed complementation studies of *atsec62* with a construct coding for *AtSEC62–ΔTMD3/C* (compare with Figures 3 and 6a) driven by the endogenous promoter. We identified two lines of homozygous mutant plants carrying the respective construct, *pAtSEC62::AtSEC62–ΔTMD3/C #30-23* and *pAtSEC62::AtSEC62–ΔTMD3/C #12-22* (Figure 6b). Strikingly, the *atsec62* phenotype was not rescued in these lines (Figure 6c,d), demonstrating that AtSec62–ΔTMD3/C cannot complement *atsec62* and thereby indicating an essential role of the AtSec62 C-terminus in *Arabidopsis*. The presence of respective *AtSEC62–ΔTMD3/C* transcripts was confirmed by RT-PCR (Figure 6e), proving that the observed phenotype was not caused by lack of gene expression.

DISCUSSION

In this study, we demonstrated that AtSec62 has three transmembrane domains and is critical for plant growth and male fertility in *Arabidopsis*. Moreover, the luminal exposed C-terminus is crucial for AtSec62 function and probably acquired a unique function in protein translocation into the ER, which was also indicated by unsuccessful complementation in yeast and sequence comparison with other Sec62 homologues.

The isolated *atsec62* T-DNA insertion line displayed delayed pollen development and impaired pollen tube germination leading to defects in male transmission. This phenotype resembles other mutant lines possessing a defective secretory pathway (Jakobsen *et al.*, 2005; Yamamoto *et al.*, 2008; Conger *et al.*, 2011; Maruyama *et al.*, 2014; Vu *et al.*, 2017). For example, *aterdj2a* and *atsec24a-1* display drastic defects in pollen germination leading to male sterility (Yamamoto *et al.*, 2008; Conger *et al.*, 2011). AtSEC24A is probably part of the COPII coat thereby playing an important role in the secretory pathway in plants by being involved in selective cargo binding during ER export (Kuehn *et al.*, 1998; Conger *et al.*, 2011). The quadruple mutant *cnx1 crt1 crt2 crt3*, lacking ER resident calreticulin and calnexin, both involved in protein quality control, shows reduced fertility due to reduced pollen viability and tube growth (Vu *et al.*, 2017). Moreover, fusion of polar nuclei in female gametophytes and pollen tube growth in *bip1 bip2* are affected, whereas *bip1 bip2 bip3* pollen are not even viable (Maruyama *et al.*, 2010, 2014). Jakobsen *et al.* (2005) showed that MIA, involved in vesicle trafficking from the ER to the plasma membrane, is required for proper protein secretion and *mia-1* has smaller leaves in
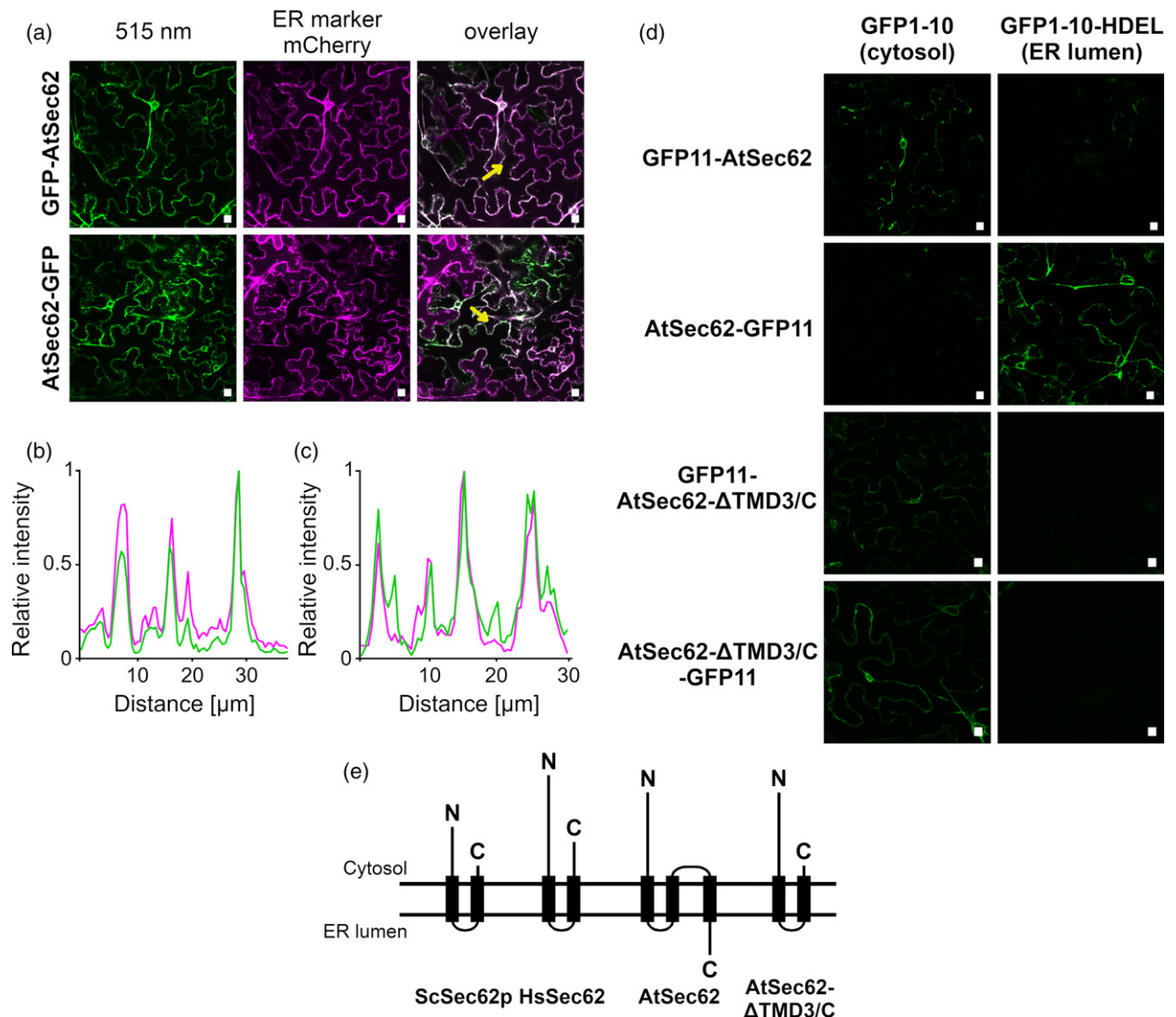
Figure 4. AtSec62 localization and topology. (a) Tobacco leaves were co-transformed with *Agrobacterium* carrying constructs for GFP−AtSec62 or AtSec62−GFP and an ER marker (mCherry). Fluorescent signals were detected by confocal microscopy in intact leaves. Scale bars represent 10 μm. Line histograms along the yellow arrow, indicated in the overlay images in (a), depicting the relative fluorescence intensity of GFP−AtSec62 (b) or AtSec62−GFP (c) as well as the ER marker. (d) Fluorescent signals were monitored in tobacco leaves expressing either GFP11−AtSec62, AtSec62−GFP11, GFP11−AtSec62-ΔTMD3/C or AtSec62−ΔTMD3/C−GFP11 and cytosolic GFP1−10 or ER luminal GFP1−10−HDEL. Scale bars represent 10 μm. (e) Topology model for AtSec62 and AtSec62−ΔTMD3/C in comparison with yeast Sec62p (ScSec62p) and human Sec62 (HsSec62).

comparison with wild-type plants and defective pollen which are not released and not germinating *in vitro* leading to reduced fertility. *mia-1* still harbours remnants of the pollen mother cell and the callosic wall attached to pollen grains preventing proper development and release of the pollen (Jakobsen *et al.*, 2005). Degradation of callose and the pollen mother cell wall is indispensable for male gametophyte development and depends on proper secretion from tapetal cells (Stieglitz, 1977; Rhee *et al.*, 2003; Lu *et al.*, 2014). Huang *et al.* (2013) have previously shown that lipid transfer proteins, which are secreted from the tapetum to become part of the microspore surface, are

required for pollen exine formation. We assume that the lack of AtSec62 not only disturbs ER protein translocation of various polypeptides but subsequently also leads to defects in secretion during vegetative growth and male gametophyte development as already proposed for AtERdj2A by Yamamoto *et al.* (2008). Defective pollen development and reduced seed germination match the *AtSEC62* expression pattern with the highest expression level observed in mature pollen and higher expression in seeds and during anther development than in vegetative tissue (*Arabidopsis* eFP browser, http://bar.utoronto.ca/, Winter *et al.*, 2007). The altered root morphology in
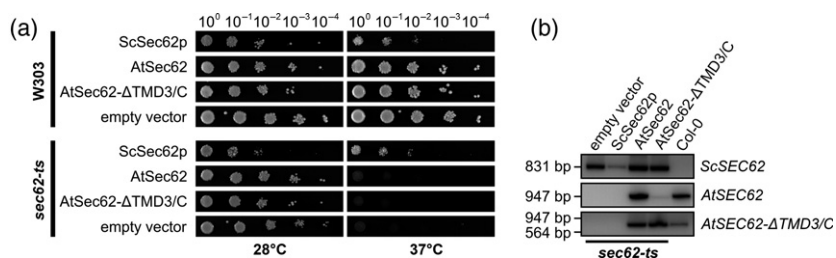
Figure 5. Complementation analysis in the thermosensitive yeast mutant *sec62-ts*. (a) Wild-type yeast (W303) and the thermosensitive yeast mutant *sec62-ts* were transformed with constructs for expression of yeast Sec62p (ScSec62p), AtSec62, AtSec62−ΔTMD3/C or the empty vector control. Following serial dilution and dropping onto solid medium plates, transformed yeast cells were grown at either a permissive (28°C) or restrictive (37°C) temperature for 48 h. (b) RT-PCR for *ScSEC62*, *AtSEC62* and *AtSEC62−ΔTMD3/C*. RNA was isolated from Col-0 plants or from *sec62-ts* yeast transformed with constructs as described in (a).

atsec62 might likewise be a result of disturbed ER protein translocation also interfering with hormone signalling and root nutrient uptake, for example regarding phosphate (compare with Pérez-Torres *et al.*, 2008; Malhotra *et al.*, 2018), which in return also affects growth of aerial plant tissues thereby contributing to the observed phenotype. However, in contrast with *aterdj2a* (Yamamoto *et al.*, 2008), we still obtained homozygous *atsec62* plants and observed *atsec62* (+/−) progeny plants not segregating in the expected ratio of 1:1 for usual gametophytic mutants. We therefore presume that the defects caused by the absence of AtSec62 can partially be bypassed or compensated by an alternative pathway.

Another *Arabidopsis* mutant line, *Atget1-1*, has a similar, though more severe vegetative phenotype in comparison with *atsec62*, when additionally overexpressing AtGET3a (Xing *et al.*, 2017). Respective plants display a dwarf phenotype, shorter roots as well as a reduced number of siliques and seeds (Xing *et al.*, 2017). AtGET1 and AtGET3a are both part of the cytosolic/ER Guided Entry of Tail-anchored proteins (GET) pathway in *Arabidopsis*, which facilitates the membrane insertion of tail-anchored proteins into the ER membrane (Srivastava *et al.*, 2017; Xing *et al.*, 2017). As no severe phenotype is observable for *Atget1-1* alone (Srivastava *et al.*, 2017; Xing *et al.*, 2017), Xing *et al.* (2017) proposed that overexpression of AtGET3a in the *Atget1-1* background caused trapping of tail-anchored proteins in the cytosol and consequently also disturbed a potential alternative insertion pathway, which might be the post-translational *Arabidopsis* Sec translocon also involving AtSec62. In *atsec62*, the GET pathway should still be functional and we speculate that it might therefore partially compensate the lack of AtSec62 in post-translational translocation and insertion of membrane proteins explaining the less severe vegetative growth phenotype in comparison with plants overexpressing AtGET3a in the *Atget1-1* background. We assume that the GET pathway might be more root specific, reflected by the root hair phenotype only observable for *Atget1-1* but not for *atsec62* (Xing *et al.*, 2017; Figure S1d). Moreover, the GET pathway can probably not compensate for lack of AtSec62

regarding the protein import of pre-secretory proteins resulting in impaired growth and drastic defects during male gametophyte development in *atsec62*. However, it still remains unclear whether there are indeed several distinct, maybe even overlapping ER translocation pathways in plants.

Besides impaired growth under normal conditions, we observed that *atsec62* plants are more sensitive towards high-temperature stress than wild-type plants as shown by reduced pollen tube germination and survival after heat treatment. These observations might be due to a generally reduced fitness of *atsec62* or due to an involvement of AtSec62 in plant thermotolerance. Yet, we observed no effect of high-temperature treatment on *atsec62* seed germination rate probably due to storage compounds already being present in seeds and therefore low ER import rates, which increase during further vegetative growth. As we additionally observed a higher susceptibility towards ER stress, we assumed that AtSec62 might also be involved in the unfolded protein response in plants (reviewed by Strasser, 2018), probably by translocating respective components across or into the ER membrane. However, it might also play a more substantial role during ER stress (recovery) similar to its mammalian homologues (Linxweiler *et al.*, 2013; Fumagalli *et al.*, 2016).

Former studies have already pointed out the low homology between AtSec62 and Sec62p as well as mammalian Sec62 (Schweiger and Schwenkert, 2013), especially regarding the diverse C-terminus which features potential N-glycosylation sites in plants, indicating exposition to the ER lumen rather than the cytosol. Indeed, we demonstrated that AtSec62 has a third transmembrane domain in contrast to its yeast and mammalian homologues (Deshaies and Schekman, 1989, 1990; Müller *et al.*, 2010) resulting in the AtSec62 C-terminus facing the ER lumen. As AtSec62−ΔTMD3/C is not sufficient for proper AtSec62 function as shown by unsuccessful complementation in *atsec62*, we propose that the C-terminus plays an essential role in protein translocation into the ER, maybe by interacting with other Sec translocon components or even translocation substrates. Identifying additional AtSec62
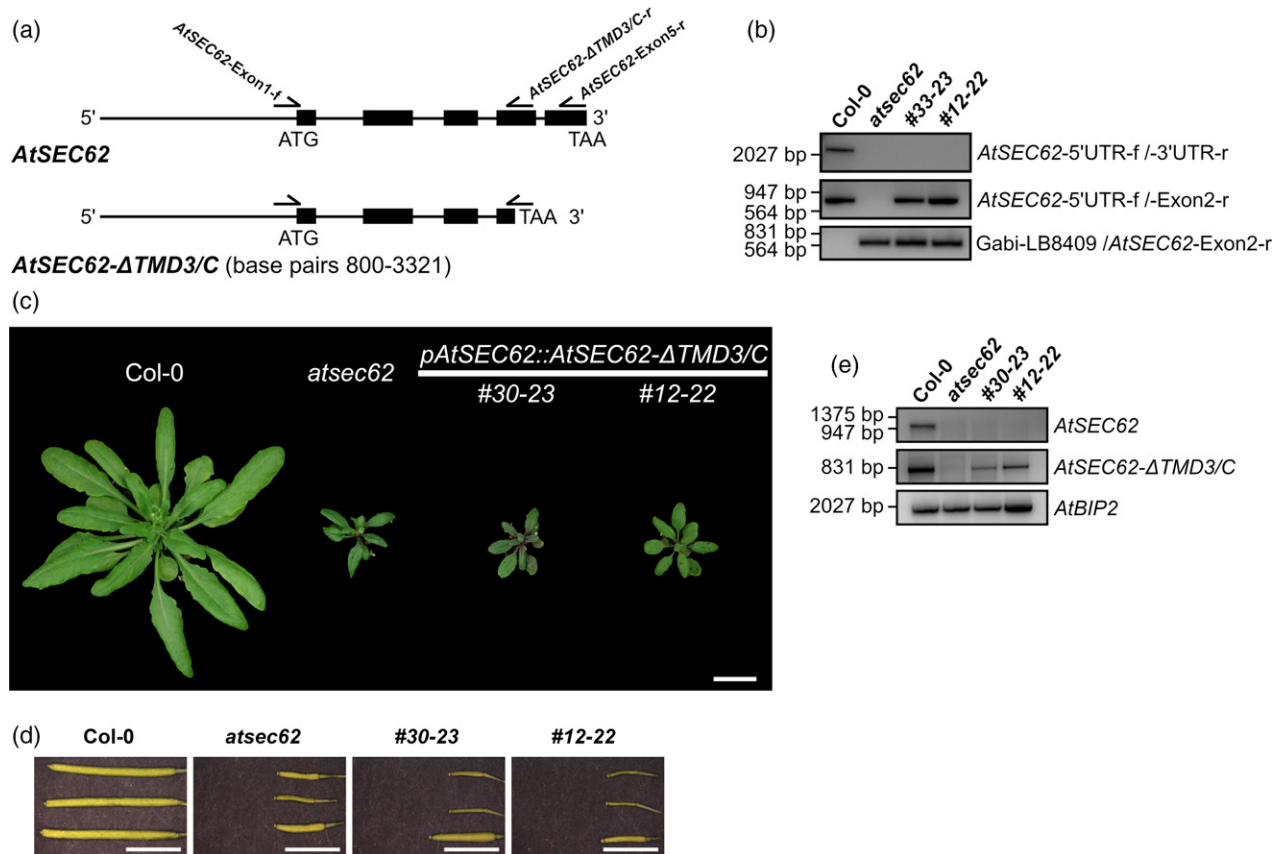
Figure 6. *atsec62* complementation analysis using *AtSEC62–ΔTMD3/C*. (a) Scheme of *AtSEC62* and *AtSEC62–ΔTMD3/C* constructs used for complementation analysis. (b) Genotyping PCR using the oligonucleotides *AtSEC62*-5′UTR-f, *AtSEC62*-Exon2-r and Gabi-LB8409. Oligonucleotide binding sites in *AtSEC62* are indicated in Figure 1(a). (c) Phenotyping of 5-week-old Col-0 and *atsec62* plants in comparison with *atsec62* lines carrying a construct for *AtSEC62–ΔTMD3/C* expression, *pAtSEC62::AtSEC62–ΔTMD3/C #30-23* (*#30-23*) and *pAtSEC62::AtSEC62–ΔTMD3/C #12-22* (*#12-22*). Scale bar represents 2 cm. (d) Siliques of Col-0 and *atsec62* in comparison with lines *#30-23* and *#12-22*. Scale bars represent 5 mm. (e) RT-PCR for *AtSEC62* or *AtSEC62–ΔTMD3/C* and the control *AtBIP2*. Oligonucleotide binding sites for *AtSEC62*-Exon1-f, *AtSEC62*-ΔTMD3/C-r and *AtSEC62*-Exon5-r in *AtSEC62* or *AtSEC62–ΔTMD3/C* are indicated in (a).

interaction partners besides AtTPR7 (Schweiger and Schwenkert, 2013) within the Sec translocation complex or beyond will be a challenging task in the future providing further insights into ER protein translocation in *Arabidopsis* thereby also explaining the observed *atsec62* phenotype. In addition, future studies might reveal whether AtSec62, similar to Sec62p (compare with Panzner *et al.*, 1995), functions solely in the post-translational translocation pathway or also contributes to the co-translational pathway as proposed for mammalian Sec62 (Müller *et al.*, 2010).

We showed that AtSec62 as well as AtSec62–ΔTMD3/C cannot rescue the thermosensitive growth phenotype of the yeast mutant *sec62-ts* in contrast to the endogenous Sec62p, whereas recent studies by Zhou *et al.* (2016) have proven that Sec62 is conserved at least in other fungal species like the phytopathogen *Magnaporthe oryzae* with MoSec62 restoring growth of thermosensitive *Δsec62* yeast. Human and *Drosophila* Sec62 homologues were also able to complement respective yeast mutants

(Noël and Cartwright, 1994; Müller *et al.*, 2010). Due to the cytosol exposed C-terminus of Sec62p having an essential function in yeast, probably by contributing to signal peptide recognition (Deshaies and Schekman, 1990; Wittke *et al.*, 2000), AtSec62 as well as AtSec62-ΔTMD3/C might be unable to restore growth of *sec62-ts*, even though AtSec62-ΔTMD3/C topology resembles the one of Sec62p. This might also be due to their inability to form proper complexes with other components of the yeast Sec translocon as already proposed by Yamamoto *et al.* (2008) after performing complementation analysis of *sec63-1* yeast mutants using AtERdj2A. AtERdj2A and AtERdj2B display only around 20% sequence identity to their yeast and human counterparts, similar to AtSec62 sharing only 12% and 15% sequence identity with Sec62p and human Sec62 (Yamamoto *et al.*, 2008; Schweiger and Schwenkert, 2013). Even regarding the predicted Sec62 domain (compare with Schweiger and Schwenkert, 2013), AtSec62 shows only 14% sequence identity with its yeast and human homologues.

Notably, also yeast Sec62p and the well studied human Sec62 share only 19% sequence identity with respect to the conserved Sec62 domain.

Summarizing, presented findings support the idea of plant Sec62 having acquired a unique function during evolution. Although we prove the importance of the luminal exposed AtSec62 C-terminus, especially in plant male fertility, its exact function in ER protein translocation still remains unclear and will be an interesting issue to address in future studies.

EXPERIMENTAL PROCEDURES

Plant material and growth conditions

Wild-type *A. thaliana* (ecotype Columbia, Col-0) and the *atsec62* T-DNA insertion line were grown on soil either under greenhouse conditions or in the climate chamber under a 16 h light/8 h dark cycle at 22°C/18°C and 100 µmol photons m^{-2} sec^{-1}. Plants for segregation analysis and high-temperature treatment were grown on ½MS medium (pH 5.7) with or without 10 µg ml^{-1} sulfadiazine, additionally containing vitamins, 1% sucrose and 0.6% (w/v) Gelrite, whereas plants for root analysis were grown on ½MS medium (pH 5.7) and 1.0% (w/v) Phytoagar, additionally supplemented with DTT (1.5 mM, 2 mM) for ER stress treatment. Seeds were sterilized (70% (v/v) ethanol, 0.05% (v/v) Triton X-100), prior to three times washing in 100% (v/v) ethanol. Seeds were stratified at 4°C for 2–3 days in the dark. For complementation analysis, we generated constructs under the control of the endogenous promoter (base pairs 800-1899 of genomic *AT3G20920*), which was narrowed down by using PlantPAN2.0 (http://plantpan2.itps.ncku.edu.tw/), coding for the full-length genomic *AtSEC62* or the truncated *AtSEC62–ΔTMD3/C* (amino acids 1–247). Stable transformation of *Arabidopsis* plants was conducted by floral dip according to Clough and Bent (1998) using *Agrobacterium tumefaciens* GV3101. *Nicotiana benthamiana* was grown in soil under greenhouse conditions.

The *atsec62* T-DNA insertion line (GK-871A06) was obtained from the European Arabidopsis Stock Centre (http://arabidopsis.info/). Homozygous mutant plants were identified by PCR using the oligonucleotides *AtSEC62*-5′UTR-f (5′-CTTGAAATGTGAGAAAAAT GAAATAC-3′), *AtSEC62*-Exon2-r (5′-ATCGTCTGTGTCAAGGTCTTT ATC-3′) and Gabi-LB8409 (5′-ATATTGACCATCATACTCATTGC-3′). For complementation analysis *AtSEC62*-3′UTR-r (5′-GAATACTTC AGATGTTGCCAC-3′) was used to distinguish between wild-type and mutant plants carrying respective constructs.

RNA extraction and RT-PCR analysis

RNA was isolated from leaves of 4- to 5-week-old plants or from 10 ml overnight yeast cultures using the RNeasy (Plant) Mini Kit (Qiagen, https://www.qiagen.com) according to manufacturer's instructions, however 2 mg ml^{-1} zymolase was used for generation of spheroplasts and DNase I digest was performed for 30 min at RT. cDNA was synthesized using the M-MLV reverse transcriptase (Promega, https://www.promega.com). Subsequent reverse transcription PCR (RT-PCR) was performed using the oligonucleotides *AtSEC62*-Exon1-f (5′-ATGAAGAAGCCGGTCGGAGCCG AG-3′), *AtSEC62*-Exon5-r (5′-TTATGTTTTAAGATCAGAGTCAGTC C-3′), *AtSEC62*-ΔTMD3/C-r (5′-GGGGACCACTTTGTACAAGAAAGC TGGGTCTTAGTCTTTCTTTGGCCAGAAAC-3′), *AtSEC62*-stop-r (5′-GGGGACCACTTTGTACAAGAAAGCTGGGTCTTATGTT-3′), *AtSEC 62–ΔTMD3/C*-no-stop-r (5′-CGATCTCGAGGTCTTTCTTTGGCCAG

AAAC-3′), *AtBIP2*-ATG-f (5′-GTACGGGCCCATGGCTCGCTCGTTTG GAG-3′), *AtBIP2*-no-stop-r (5′-GTACGCGGCCGCAGAGCTCATCG TGAGACTCATC-3′) as well as *ScSEC62*-for (5′-GGGGACAAGTTT GTACAAAAAAGCAGGCTATGTCAGCCGTAGGTCCAGG-3′) and *ScSEC62*-rev (5′-GGGGACCACTTTGTACAAGAAGCTGGGTCTCA GTTTTGTTCGGCTTTTTC-3′).

Preparation of microsomal membranes

Microsomal membranes were prepared from 4-week-old *Arabidopsis* plants. All steps were carried out at 4°C. Plant material was frozen in liquid nitrogen, ground in 50 mM Tris–HCl (pH 7.5), 2 mM MgCl$_2$, 100 mM KCl and 0.5 M sucrose and filtered through gauze. To remove chloroplasts and mitochondria, the plant lysate was centrifuged once at 4 200 *g* for 10 min, at 10 000 *g* for 10 min and at 22 000 *g* for 30 min. To pellet microsomal membranes the remaining supernatant was centrifuged at 100 000 *g* for 1 h. For further purification of microsomal membranes, the resulting pellet was resuspended in 50 mM Tris–HCl (pH 7.5), 2 mM MgCl$_2$, 100 mM KCl and 12% (w/v) sucrose, loaded onto a step gradient (50%, 30% and 20% sucrose) and centrifuged at 100 000 *g* for 1 h. The fraction between 50% and 30% sucrose was transferred to a new tube and washed once at 100 000 *g* for 1 h. Microsomal membranes were resuspended in 25 mM Tris–HCl (pH 7.5), 0.33 M sucrose and 0.5 mM DTT.

SDS-PAGE and immunoblotting

Proteins were separated on 12% polyacrylamide. Subsequently, proteins were transferred onto PVDF membranes by semi-dry blotting and immunodetection was visualized using enhanced chemiluminescence. AtSec62 antibody was raised against the recombinant AtSec62 N-terminus (amino acids 1–160) fused to a C-terminal His-tag and was generated in rabbits by BioGenes (https://www.biogenes.de/).

Pollen staining and germination assay

Alexander staining solution was prepared according to Alexander (1969). For *in vitro* pollen germination assays, pollen grains from 8-week-old plants were spread onto solidified germination medium (1 mM MgCl$_2$, 0.16 mM H$_3$BO$_3$, 1 mM CaCl$_2$, 1 mM Ca(NO$_3$)$_2$, 18% sucrose (w/v), 0.65% (w/v) Phytoagar) and incubated for 22 h at high humidity in the dark at 25°C and 37°C.

Agrobacterium-mediated transient expression of fluorescent proteins in tobacco

Infiltration of leaves from 4- to 6-week-old *Nicotiana benthamiana* plants, isolation of protoplasts and subsequent detection of fluorescence signals were performed as described previously (Koop et al., 1996; Schweiger and Schwenkert, 2014). However, cell cultures of *Agrobacterium tumefaciens* Agl1 carrying respective constructs were resuspended in infiltration medium containing 10 mM MgCl$_2$, 10 mM MES (pH 6) but only 100 µM acetosyringone. For transient expression of respective fluorescent proteins, leaves of *Nicotiana benthamiana* were infiltrated with *Agrobacterium*. Fluorescence signals in leaves or isolated protoplasts were detected after 2–3 days of incubation by confocal laser scanning microscopy (Leica TCS SP5 CLSM, imaging medium: glycerol, Software: Leica Application Suite/Advanced Fluorescence) at RT (compare with Schweiger and Schwenkert, 2014). For localization and topology studies, the *AtSEC62* or *AtSEC62–ΔTMD3/C* coding region was cloned into the binary Gateway vectors pB7FWG2 and

pK7WGF2 (Karimi *et al.*, 2002) or the appropriate Split-GFP Gateway vectors (Xie *et al.*, 2017). The constructed Split-GFP plasmids encode the GFP β-sheets 1−10 (compare with Cabantous *et al.*, 2005) being expressed either in the cytosol (GFP1−10) or in the ER lumen by an integrated ER retention signal (GFP1−10−HDEL) (Xie *et al.*, 2017). The Gateway vectors also facilitate N- or C-terminal fusion of the eleventh β-sheet to AtSec62 (compare with Xie *et al.*, 2017). The C-terminal *AtSEC62−ΔTMD3/C* fusion construct contained an additional C-terminal His-tag. The ER marker has been described recently (Nelson *et al.*, 2007; Schweiger *et al.*, 2012).

Yeast strains and complementation analysis

Complementation analysis in yeast was performed using the wild-type strain W303 and the thermosensitive mutant *sec62-ts* (BY4741; *MATα*; *ura3Δ0*; *leu2Δ0*; *his3Δ1*; *met15Δ0*; *sec62-ts: kanMX*; obtained from EUROSCARF, http://euroscarf.de/). Yeast cells were grown in YPD medium (1% (w/v) bacto yeast extract, 2% (w/v) bacto peptone, 2% (w/v) glucose) or in SCD medium (0.7% (w/v) yeast nitrogen base without amino acids, 2% (w/v) glucose, 0.2% (w/v) dropout mix without leucine). Solid media were supplemented with 2% (w/v) bacto agar. For complementation analysis, the yeast *SEC62* and *AtSEC62* coding region were cloned into the Gateway vector pAG425GPD-ccdB (Alberti *et al.*, 2007). Yeast genomic DNA was isolated as previously described (Lõoke *et al.*, 2011), however, 70% (v/v) ethanol was used for DNA precipitation.

Competent yeast cell preparation and subsequent transformation were modified based on Staudinger *et al.* (1995). For generation of competent cells, yeast cells were grown in 50 ml YPD medium at 30°C and cells were harvested at OD_{600} 0.5–0.6 by centrifugation for 5 min at 700 *g* and 4°C. Cells were washed in 50 ml sterile water, prior to washing in 12.5 ml LiSorb (100 mᴍ LiOAc, 10 mᴍ Tris−HCl pH 8, 1 mᴍ ethylene diamine tetraacetic acid (EDTA) pH 8, 1 M sorbitol). Yeast cells were subsequently resuspended in 300 µl LiSorb and 42 µl carrier DNA (2 mg ml^{-1} denatured and sheared herring sperm DNA) were added. For yeast transformation, 5 µl plasmid DNA and 300 µl LiPEG (100 mᴍ LiOAc, 10 mᴍ Tris−HCl pH 8, 1 mᴍ EDTA pH 8, 40% (w/v) PEG 3350) were added to 50 µl competent cells and the mixture was incubated for 20 min at RT. 35 µl dimethyl sulphoxide (DMSO) were added prior to a heat shock at 42°C for 15 min. Yeast cells were pelleted at 700 *g* for 90 sec, resuspended in 0.9% (w/v) NaCl and spread on SCD medium plates. Yeast transformants were then grown in SCD medium at 30°C, OD_{600} was adjusted to 1.0 and serial dilutions of each strain were spotted onto SCD medium plates. Yeast cells were then grown for 48 h at 28°C or 37°C.

Sequence analysis

Transmembrane domains of Sec62 homologues were defined based on predictions by TMHMM2.0 (http://www.cbs.dtu.dk/services/TMHMM/), TMpred (https://embnet.vital-it.ch/software/TMPRED_form.html), Phobius (http://phobius.sbc.su.se/) and DAS-TMfilter (http://www.enzim.hu/DAS/DAS.html). The conserved Sec62 domain was identified using NCBI Conserved Domain Search (https://www.ncbi.nlm.nih.gov/Structure/cdd/wrpsb.cgi). Alignments were generated using ClustalW software.

Statistical analysis

Chi-squared test was used to assess deviations of the observed segregation pattern from the expected Mendelian ratios, whereas root and seed yield analysis were performed using Student's *t*-test (two-sided, equal variance). The significance threshold was set at $P \leq 0.05$. Box plots were generated using BoxPlotR software (http://shiny.chemgrid.org/boxplotr/).

ACCESSION NUMBERS

Sequence data used in this study can be found in the NCBI data libraries (https://www.ncbi.nlm.nih.gov/) under following accession numbers: At3g20920 (AtSec62), XP_015627309 (*Oryza sativa* Sec62), XP_008681002 (*Zea mays* Sec62), XP_024398141 (*Physcomitrella patens* Sec62), XP_001701717 (*Chlamydomonas reinhardtii* Sec62), NP_003253 (*Homo sapiens* Sec62), NP_081292 (*Mus musculus* Sec62), NP_015231 (*Saccharomyces cerevisiae* Sec62p) and XP_017075746 (*Drosophila eugracilis* Sec62) as well as At5g42020 (AtBiP2).

CONFLICT OF INTEREST

The authors declare no conflict of interest.

AUTHORS' CONTRIBUTIONS

MJM conducted and analyzed experiments, participated in designing experiments and wrote the manuscript. FAB and TB performed experiments; FAB analyzed experiments. SS supervised the study, conceived experiments and revised the manuscript. All authors read and approved the final version of the manuscript.

SUPPORTING INFORMATION

Additional Supporting Information may be found in the online version of this article.

Figure S1. Root morphology of *atsec62* in comparison to Col-0.

Figure S2. *atsec62* sensitivity towards ER stress.

Figure S3. Amino acid sequence alignment of Sec62 homologues.

Figure S4. Localization of AtSec62 GFP-fusion constructs in tobacco protoplasts.

Figure S5. Expression of AtSec62 Split-GFP constructs in isolated tobacco protoplasts.

REFERENCES

Alberti, S., Gitler, A.D. and Lindquist, S. (2007) A suite of Gateway cloning vectors for high-throughput genetic analysis in *Saccharomyces cerevisiae. Yeast*, **24**, 913–919. https://doi.org/10.1002/yea.1502.

Alexander, M.P. (1969) Differential staining of aborted and nonaborted pollen. *Stain Technol.*, **44**, 117–122. https://doi.org/10.3109/10520296909063335.

Ast, T. and Schuldiner, M. (2013) All roads lead to Rome (but some may be harder to travel): SRP-independent translocation into the endoplasmic reticulum. *Crit. Rev. Biochem. Mol. Biol.* **48**, 273–288. https://doi.org/10.3109/10409238.2013.782999

Brodsky, J.L. and Schekman, R. (1993) A Sec63p-BiP complex from yeast is required for protein translocation in a reconstituted proteoliposome. *J. Cell Biol.* **123**, 1355–1363. https://doi.org/10.1083/jcb.123.6.1355

Brodsky, J.L., Goeckeler, J. and Schekman, R. (1995) BiP and Sec63p are required for both co- and posttranslational protein translocation into the yeast endoplasmic reticulum. *Proc. Natl Acad. Sci. USA*, **92**, 9643–9646. https://doi.org/10.1073/pnas.92.21.9643

Cabantous, S., Terwilliger, T.C. and Waldo, G.S. (2005) Protein tagging and detection with engineered self-assembling fragments of green fluorescent protein. *Nat. Biotechnol.* **23**, 102–107. https://doi.org/10.1038/nbt1044

Clough, S.J. and Bent, A.F. (1998) Floral dip: a simplified method for Agrobacterium-mediated transformation of *Arabidopsis thaliana*. *Plant J.* **16**, 735–743. https://doi.org/10.1046/j.1365-313x.1998.00343.x

Conger, R., Chen, Y., Fornaciari, S., Faso, C., Held, M.A., Renna, L. and Brandizzi, F. (2011) Evidence for the involvement of the Arabidopsis SEC24A in male transmission. *J. Exp. Bot.* **62**, 4917–4926. https://doi.org/10.1093/jxb/err174

Cross, B.C., Sinning, I., Luirink, J. and High, S. (2009) Delivering proteins for export from the cytosol. *Nat. Rev. Mol. Cell Biol.* **10**, 255–264. https://doi.org/10.1038/nrm2657

Deshaies, R.J. and Schekman, R. (1989) SEC62 encodes a putative membrane protein required for protein translocation into the yeast endoplasmic reticulum. *J. Cell Biol.* **109**, 2653–2664. https://doi.org/10.1083/jcb.109.6.2653

Deshaies, R.J. and Schekman, R. (1990) Structural and functional dissection of Sec62p, a membrane-bound component of the yeast endoplasmic reticulum protein import machinery. *Mol. Cell. Biol.* **10**, 6024–6035. https://doi.org/10.1128/MCB.10.11.6024

Deshaies, R.J., Sanders, S.L., Feldheim, D.A. and Schekman, R. (1991) Assembly of yeast Sec proteins involved in translocation into the endoplasmic reticulum into a membrane-bound multisubunit complex. *Nature*, **349**, 806–808. https://doi.org/10.1038/349806a0.

Drews, G.N. and Koltunow, A.M. (2011) The female gametophyte. *Arabidopsis Book*, **9**, e0155. https://doi.org/10.1199/tab.0155

Fang, H. and Green, N. (1994) Nonlethal sec71-1 and sec72-1 mutations eliminate proteins associated with the Sec63p-BiP complex from *S. cerevisiae*. *Mol. Biol. Cell*, **5**, 933–942. https://doi.org/10.1091/mbc.5.9.933.

Feldheim, D. and Schekman, R. (1994) Sec72p contributes to the selective recognition of signal peptides by the secretory polypeptide translocation complex. *J. Cell Biol.* **126**, 935–943. https://doi.org/10.1083/jcb.126.4.935

Fumagalli, F., Noack, J., Bergmann, T.J. *et al.* (2016) Translocon component Sec62 acts in endoplasmic reticulum turnover during stress recovery. *Nat. Cell Biol.* **18**, 1173–1184. https://doi.org/10.1038/ncb3423

Harada, Y., Li, H., Wall, J.S., Li, H. and Lennarz, W.J. (2011) Structural studies and the assembly of the heptameric post-translational translocon complex. *J. Biol. Chem.* **286**, 2956–2965. https://doi.org/10.1074/jbc.M110.159517

Huang, M.-D., Chen, T.-L. and Huang, A.H. (2013) Abundant type III lipid transfer proteins in Arabidopsis tapetum are secreted to the locule and become a constituent of the pollen exine. *Plant Physiol.* **163**, 1218–1229. https://doi.org/10.1104/pp.113.225706

Itskanov, S. and Park, E. (2019) Structure of the posttranslational Sec protein-translocation channel complex from yeast. *Science*, **363**, 84–87. https://doi.org/10.1126/science.aav6740

Jakobsen, M.K., Poulsen, L.R., Schulz, A., Fleurat-Lessard, P., Møller, A., Husted, S., Schiøtt, M., Amtmann, A. and Palmgren, M.G. (2005) Pollen development and fertilization in Arabidopsis is dependent on the MALE GAMETOGENESIS IMPAIRED ANTHERS gene encoding a type V P-type ATPase. *Genes Dev.* **19**, 2757–2769. https://doi.org/10.1101/gad.357305

Jung, S.J., Kim, J.E., Reithinger, J.H. and Kim, H. (2014) The Sec62-Sec63 translocon facilitates translocation of the C-terminus of membrane proteins. *J. Cell Sci.* **127**, 4270–4278. https://doi.org/10.1242/jcs.153650

Jung, S.J., Jung, Y. and Kim, H. (2019) Proper insertion and topogenesis of membrane proteins in the ER depend on Sec63. *Biochim. Biophys. Acta Gen. Subj.* **1863**, 1371–1380. https://doi.org/10.1016/j.bbagen.2019.06.005

Karimi, M., Inzé, D. and Depicker, A. (2002) GATEWAY vectors for Agrobacterium-mediated plant transformation. *Trends Plant Sci.* **7**, 193–195. https://doi.org/10.1016/S1360-1385(02)02251-3

Koop, H.-U., Steinmüller, K., Wagner, H., Rößler, C., Eibl, C. and Sacher, L. (1996) Integration of foreign sequences into the tobacco plastome via polyethylene glycol-mediated protoplast transformation. *Planta*, **199**, 193–201. https://doi.org/10.1007/BF00196559

Kuehn, M.J., Herrmann, J.M. and Schekman, R. (1998) COPII-cargo interactions direct protein sorting into ER-derived transport vesicles. *Nature*, **391**, 187–190. https://doi.org/10.1038/34438

Lakkaraju, A.K., Thankappan, R., Mary, C., Garrison, J.L., Taunton, J. and Strub, K. (2012) Efficient secretion of small proteins in mammalian cells relies on Sec62-dependent posttranslational translocation. *Mol. Biol. Cell*, **23**, 2712–2722. https://doi.org/10.1091/mbc.E12-03-0228.

Lang, S., Benedix, J., Fedeles, S.V. *et al.* (2012) Different effects of Sec61alpha, Sec62 and Sec63 depletion on transport of polypeptides into the endoplasmic reticulum of mammalian cells. *J. Cell Sci.* **125**, 1958–1969. https://doi.org/10.1242/jcs.096727

Linxweiler, M., Schorr, S., Schäuble, N., Jung, M., Linxweiler, J., Langer, F., Schäfers, H.J., Cavaliè, A., Zimmermann, R. and Greiner, M. (2013) Targeting cell migration and the endoplasmic reticulum stress response with calmodulin antagonists: a clinically tested small molecule phenocopy of SEC62 gene silencing in human tumor cells. *BMC Cancer*, **13**, 574. https://doi.org/10.1186/1471-2407-13-574

Linxweiler, M., Schick, B. and Zimmermann, R. (2017) Let's talk about Secs: Sec61, Sec62 and Sec63 in signal transduction, oncology and personalized medicine. *Signal Transduct. Target Ther.* **2**, 17002. https://doi.org/10.1038/sigtrans.2017.2

Liu, J. and Qu, L.-J. (2008) Meiotic and mitotic cell cycle mutants involved in gametophyte development in Arabidopsis. *Mol. Plant* **1**, 564–574. https://doi.org/10.1093/mp/ssn033

Lõoke, M., Kristjuhan, K. and Kristjuhan, A. (2011) Extraction of genomic DNA from yeasts for PCR-based applications. *Biotechniques*, **50**, 325–328. https://doi.org/10.2144/000113672

Lu, P., Chai, M., Yang, J., Ning, G., Wang, G. and Ma, H. (2014) The Arabidopsis CALLOSE DEFECTIVE MICROSPORE1 gene is required for male fertility through regulating callose metabolism during microsporogenesis. *Plant Physiol.* **164**, 1893–1904. https://doi.org/10.1104/pp.113.233387

Lyman, S.K. and Schekman, R. (1997) Binding of secretory precursor polypeptides to a translocon subcomplex is regulated by BiP. *Cell*, **88**, 85–96. https://doi.org/10.1016/s0092-8674(00)81861-9

Malhotra, H., Vandana, X., Sharma, S. and Pandey, R. (2018). Phosphorus nutrition: plant growth in response to deficiency and excess. In *Plant Nutrients and Abiotic Stress Tolerance* (Hasanuzzaman, M., Fujita, M., Oku, H., Nahar, K. and Hawrylak-Nowak, B., eds). Singapore: Springer Nature, pp. 171–190. https://doi.org/10.1007/978-981-10-9044-8_7

Marshall, R.D. (1972) Glycoproteins. *Ann. Rev. Biochem.* **41**, 673–702. https://doi.org/10.1146/annurev.bi.41.070172.003325

Martínez-Gil, L., Saurí, A., Marti-Renom, M.A. and Mingarro, I. (2011) Membrane protein integration into the endoplasmic reticulum. *FEBS J.* **278**, 3846–3858. https://doi.org/10.1111/j.1742-4658.2011.08185.x

Maruyama, D., Endo, T. and Nishikawa, S. (2010) BiP-mediated polar nuclei fusion is essential for the regulation of endosperm nuclei proliferation in *Arabidopsis thaliana*. *Proc. Natl Acad. Sci. USA*, **107**, 1684–1689. https://doi.org/10.1073/pnas.0905795107

Maruyama, D., Sugiyama, T., Endo, T. and Nishikawa, S. (2014) Multiple BiP genes of *Arabidopsis thaliana* are required for male gametogenesis and pollen competitiveness. *Plant Cell Physiol.* **55**, 801–810. https://doi.org/10.1093/pcp/pcu018

Meyer, H.-A., Grau, H., Kraft, R., Kostka, S., Prehn, S., Kalies, K.-U. and Hartmann, E. (2000) Mammalian Sec61 is associated with Sec62 and Sec63. *J. Biol. Chem.* **275**, 14550–14557. https://doi.org/10.1074/jbc.275.19.14550

Müller, L., de Escauriaza, M.D., Lajoie, P. *et al.* (2010) Evolutionary gain of function for the ER membrane protein Sec62 from yeast to humans. *Mol. Biol. Cell*, **21**, 691–703. https://doi.org/10.1091/mbc.E09-08-0730

Nelson, B.K., Cai, X. and Nebenführ, A. (2007) A multicolored set of in vivo organelle markers for co-localization studies in Arabidopsis and other plants. *Plant J.* **51**, 1126–1136. https://doi.org/10.1111/j.1365-313X.2007.03212.x

Ng, D.T., Brown, J.D. and Walter, P. (1996) Signal sequences specify the targeting route to the endoplasmic reticulum membrane. *J. Cell Biol.* **134**, 269–278. https://doi.org/10.1083/jcb.134.2.269

Ngosuwan, J., Wang, N.M., Fung, K.L. and Chirico, W.J. (2003) Roles of cytosolic Hsp70 and Hsp40 molecular chaperones in post-translational

translocation of presecretory proteins into the endoplasmic reticulum. *J. Biol. Chem.* **278**, 7034–7042. https://doi.org/10.1074/jbc.M210544200

Noël, P. and Cartwright, I.L. (1994) A Sec62p-related component of the secretory protein translocon from Drosophila displays developmentally complex behavior. *EMBO J.* **13**, 5253–5261. https://doi.org/10.1002/j.1460-2075.1994.tb06859.x

Osborne, A.R., Rapoport, T.A. and van den Berg, B. (2005) Protein translocation by the Sec61/SecY channel. *Annu. Rev. Cell Dev. Biol.* **21**, 529–550. https://doi.org/10.1146/annurev.cellbio.21.012704.133214

Panzner, S., Dreier, L., Hartmann, E., Kostka, S. and Rapoport, T.A. (1995) Posttranslational protein transport in yeast reconstituted with a purified complex of Sec proteins and Kar2p. *Cell*, **81**, 561–570. https://doi.org/10.1016/0092-8674(95)90077-2

Pérez-Torres, C.-A., López-Bucio, J., Cruz-Ramírez, A., Ibarra-Laclette, E., Dharmasiri, S., Estelle, M. and Herrera-Estrella, L. (2008) Phosphate availability alters lateral root development in Arabidopsis by modulating auxin sensitivity via a mechanism involving the TIR1 auxin receptor. *Plant Cell*, **20**, 3258–3272. https://doi.org/10.1105/tpc.108.058719

Plath, K., Mothes, W., Wilkinson, B.M., Stirling, C.J. and Rapoport, T.A. (1998) Signal sequence recognition in posttranslational protein transport across the yeast ER membrane. *Cell*, **94**, 795–807. https://doi.org/10.1016/S0092-8674(00)81738-9

Rapoport, T.A. (2007) Protein translocation across the eukaryotic endoplasmic reticulum and bacterial plasma membranes. *Nature*, **450**, 663–669. https://doi.org/10.1038/nature06384

Reithinger, J.H., Kim, J.E. and Kim, H. (2013) Sec62 protein mediates membrane insertion and orientation of moderately hydrophobic signal anchor proteins in the endoplasmic reticulum (ER). *J. Biol. Chem.* **288**, 18058–18067. https://doi.org/10.1074/jbc.M113.473009.

Rhee, S.Y., Osborne, E., Poindexter, P.D. and Somerville, C.R. (2003) Microspore separation in the quartet 3 mutants of Arabidopsis is impaired by a defect in a developmentally regulated polygalacturonase required for pollen mother cell wall degradation. *Plant Physiol.* **133**, 1170–1180. https://doi.org/10.1104/pp.103.028266

Saraogi, I. and Shan, S.O. (2011) Molecular mechanism of co-translational protein targeting by the signal recognition particle. *Traffic*, **12**, 535–542. https://doi.org/10.1111/j.1600-0854.2011.01171.x

Schlegel, T., Mirus, O., von Haeseler, A. and Schleiff, E. (2007) The tetratricopeptide repeats of receptors involved in protein translocation across membranes. *Mol. Biol. Evol.* **24**, 2763–2774. https://doi.org/10.1093/molbev/msm211

Schwartz, T. and Blobel, G. (2003) Structural basis for the function of the beta subunit of the eukaryotic signal recognition particle receptor. *Cell*, **112**, 793–803. https://doi.org/10.1016/S0092-8674(03)00161-2

Schweiger, R. and Schwenkert, S. (2013) AtTPR7 as part of the *Arabidopsis* Sec post-translocon. *Plant Signal Behav.* **8**, e25286. https://doi.org/10.4161/psb.25286

Schweiger, R. and Schwenkert, S. (2014) Protein-protein interactions visualized by bimolecular fluorescence complementation in tobacco protoplasts and leaves. *J. Vis. Exp.* (85), e51327. https://doi.org/10.3791/51327

Schweiger, R., Müller, N.C., Schmitt, M.J., Soll, J. and Schwenkert, S. (2012) AtTPR7 is a chaperone-docking protein of the Sec translocon in Arabidopsis. *J. Cell Sci.* **125**, 5196–5207. https://doi.org/10.1242/jcs.111054

Schweiger, R., Soll, J., Jung, K., Heermann, R. and Schwenkert, S. (2013) Quantification of interaction strengths between chaperones and tetratricopeptide repeat domain-containing membrane proteins. *J. Biol. Chem.* **288**, 30614–30625. https://doi.org/10.1074/jbc.M113.493015

Srivastava, R., Zalisko, B.E., Keenan, R.J. and Howell, S.H. (2017) The GET system inserts the tail-anchored protein, SYP72, into endoplasmic reticulum membranes. *Plant Physiol.* **173**, 1137–1145. https://doi.org/10.1104/pp.16.00928

Staudinger, J., Zhou, J., Burgess, R., Elledge, S.J. and Olson, E.N. (1995) PICK1: a perinuclear binding protein and substrate for protein kinase C isolated by the yeast two-hybrid system. *J. Cell Biol.* **128**, 263–271. https://doi.org/10.1083/jcb.128.3.263

Stieglitz, H. (1977) Role of beta-1,3-glucanase in postmeiotic microspore release. *Dev. Biol.* **57**, 87–97. https://doi.org/10.1016/0012-1606(77)90356-6

Strasser, R. (2018) Protein quality control in the endoplasmic reticulum of plants. *Annu. Rev. Plant Biol.* **69**, 147–172. https://doi.org/10.1146/annurev-arplant-042817-040331

Tajima, S., Lauffer, L., Rath, V.L. and Walter, P. (1986) The signal recognition particle receptor is a complex that contains two distinct polypeptide chains. *J. Cell Biol.* **103**, 1167–1178. https://doi.org/10.1083/jcb.103.4.1167

Tyedmers, J., Lerner, M., Bies, C., Dudek, J., Skowronek, M.H., Haas, I.G., Heim, N., Nastainczyk, W., Volkmer, J. and Zimmermann, R. (2000) Homologs of the yeast Sec complex subunits Sec62p and Sec63p are abundant proteins in dog pancreas microsomes. *Proc. Natl Acad. Sci. USA*, **97**, 7214–7219. https://doi.org/10.1073/pnas.97.13.7214

Vu, K.V., Nguyen, N.T., Jeong, C.Y., Lee, Y.-H., Lee, H. and Hong, S.-W. (2017) Systematic deletion of the ER lectin chaperone genes reveals their roles in vegetative growth and male gametophyte development in Arabidopsis. *Plant J.* **89**, 972–983. https://doi.org/10.1111/tpj.13435

Willer, M., Jermy, A.J., Young, B.P. and Stirling, C.J. (2003) Identification of novel protein-protein interactions at the cytosolic surface of the Sec63 complex in the yeast ER membrane. *Yeast*, **20**, 133–148. https://doi.org/10.1002/yea.954

Winter, D., Vinegar, B., Nahal, H., Ammar, R., Wilson, G.V. and Provart, N.J. (2007) An "electronic fluorescent pictograph" browser for exploring and analyzing large-scale biological data sets. *PLoS ONE*, **2**, e718. https://doi.org/10.1371/journal.pone.0000718

Wittke, S., Dünnwald, M. and Johnsson, N. (2000) Sec62p, a component of the endoplasmic reticulum protein translocation machinery, contains multiple binding sites for the Sec-complex. *Mol. Biol. Cell*, **11**, 3859–3871. https://doi.org/10.1091/mbc.11.11.3859

Wu, X., Cabanos, C. and Rapoport, T.A. (2019) Structure of the post-translational protein translocation machinery of the ER membrane. *Nature*, **566**, 136–139. https://doi.org/10.1038/s41586-018-0856-x

Xie, W., Nielsen, M.E., Pedersen, C. and Thordal-Christensen, H. (2017) A split-GFP gateway cloning system for topology analyses of membrane proteins in plants. *PLoS ONE*, **12**, e0170118. https://doi.org/10.1371/journal.pone.0170118

Xing, S., Mehlhorn, D.G., Wallmeroth, N. *et al.* (2017) Loss of GET pathway orthologs in *Arabidopsis thaliana* causes root hair growth defects and affects SNARE abundance. *Proc. Natl Acad. Sci. USA*, **114**, E1544–E1553. https://doi.org/10.1073/pnas.1619525114

Yamamoto, M., Maruyama, D., Endo, T. and Nishikawa, S. (2008) *Arabidopsis thaliana* has a set of J proteins in the endoplasmic reticulum that are conserved from yeast to animals and plants. *Plant Cell Physiol.* **49**, 1547–1562. https://doi.org/10.1093/pcp/pcn119

Yang, K.-Z., Xia, C., Liu, X.-L. *et al.* (2009) A mutation in thermosensitive male sterile 1, encoding a heat shock protein with DnaJ and PDI domains, leads to thermosensitive gametophytic male sterility in Arabidopsis. *Plant J.* **57**, 870–882. https://doi.org/10.1111/j.1365-313X.2008.03732.x

Yim, C., Jung, S.J., Kim, J.E.H., Jung, Y., Jeong, S.D. and Kim, H. (2018) Profiling of signal sequence characteristics and requirement of different translocation components. *Biochim. Biophys. Acta Mol. Cell Res.* **1865**, 1640–1648. https://doi.org/10.1016/j.bbamcr.2018.08.018

Zhou, Z., Pang, Z., Li, G., Lin, C., Wang, J., Lv, Q., He, C. and Zhu, L. (2016) Endoplasmic reticulum membrane-bound MoSec62 is involved in the suppression of rice immunity and is essential for the pathogenicity of *Magnaporthe oryzae*. *Mol. Plant Pathol.* **17**, 1211–1222. https://doi.org/10.1111/mpp.12357

Zimmermann, R., Sagstetter, M., Lewis, M.J. and Pelham, H.R. (1988) Seventy-kilodalton heat shock proteins and an additional component from reticulocyte lysate stimulate import of M13 procoat protein into microsomes. *EMBO J.* **7**, 2875–2880. https://doi.org/10.1002/j.1460-2075.1988.tb03144.x

Zimmermann, R., Eyrisch, S., Ahmad, M. and Helms, V. (2011) Protein translocation across the ER membrane. *Biochim. Biophys. Acta*, **1808**, 912–924. https://doi.org/10.1016/j.bbamem.2010.06.015